Proceedings of the 3rd International Symposium on Uncertainty Quantification and Stochastic Modeling
D.A. Rade; A. M. G. Lima (Editors), ABCM, Maresias, SP, Brazil, February 15-19, 2016

State Estimation Problem in a Complex Domain: RF Hyperthermia Treatment using Nanoparticles

Leonardo Antonio Bermeo Varon [1], Helcio Rangel Barreto Orlande [1], and Guillermo Enrique Eliçabe [2]

[1] Federal University of Rio de Janeiro, Department of Mechanical Engineering, PEM/COPPE, Rio de Janeiro, RJ, Brazil

[2] University of Mar del Plata, Institute of Materials Science and Technology, INTEMA, Mar del Plata, Argentina

Abstract: The particle filter methods have been commonly used to solve inverse problems of sequential Bayesian inference in dynamic models. The particle filter methods are an approximation of sequences of probability distributions of interest, using a large set of random samples, which take into account uncertainties in the model and in the measurements. In this paper the main focus is the solution the state estimation in radiofrequency (RF) hyperthermia with nanoparticles in a complex domain. This domain contains different tissues like muscle, pancreas, lungs, duodenum and a tumor which is loaded with magnetic nanoparticles. The radiofrequency induction causes a temperature increase in the tissues, majorly in the tumor where the nanoparticles are concentrated. The results indicated an excellent agreement between estimated and exact values of temperature in the region.

Keywords: Bayesian Inference, Inverse Problem, Nanoparticles, Hyperthermia, Radiofrequency

NOMENCLATURE

C = specific heat, J/(kgK)
$\mathbf{E}$ = electric field strength, V/m
f = frequency, MHz
$\mathbf{H}$ = intensity of the magnetic field, A/m
h_f = heat transfer coefficient, W/(m^{2}K)
k = thermal conductivity, W/(mK)
n = number of nanoparticles
Q = volumetric heat source, W/m^3
r = mean radius of nanoparticles, m
T_b = blood temperature, °C
T_f = temperature of the surrounding medium, °C

Greek Symbols

ε = permittivity, dimensionless
ρ = density, kg/m^3
ω = blood perfusion rate, s^{-1}
σ = electric conductivity, S/m
χ = susceptibility of the magnetic nanoparticles, dimensionless
μ_0 = dielectric permeability constant, T·m/A

Subscripts

b = blood
e = electrical
est = estimated
exa = exact
m = metabolism

INTRODUCTION

The particle filter methods which became widely used to solve inverse problems of sequential Bayesian inference in dynamic models are of great interest for different practical applications, such as in engineering, biomedicine, economics, among others. In these applications, the available measured data are used together with prior knowledge about the physical phenomena and the measuring devices, in order to sequentially produce estimates of the desired dynamic variables (Maybeck 1979; Kaipio & Somersalo 2004).

Currently, the particle filter methods have been used in the analysis of cancer treatment (Varon et al. 2015; Lamien et al. 2014; Costa et al. 2015), providing excellent results in simples geometries. Hyperthermia is a cancer treatment where the tumor tissues heated to high temperatures, frequently between 40°C and 47°C (Miaskowski & Sawicki 2013), where the heating imposed is carried out by induction of electromagnetic waves (Ng & Jamil 2014; Dombrovsky et al. 2015). This treatment aims to kill the tumor or to make it more susceptible to the effects of radiation (Horsman & Overgaard 2007) or chemotherapy (Colombo et al. 2003). The hyperthermia treatment with nanoparticles loaded into the tumorous cells can concentrate the temperature increase to this region, thus not resulting on damages to the healthy tissues (Kurgan & Gas 2015; Paruch 2014; Varon et al. 2015; Dombrovsky et al. 2011; Lamien et al. 2014; Eibner et al. 2014).

In the present study the particle filter is applied to the hyperthermia treatment of cancer with tumorous cells loaded with nanoparticles, in domain with complex geometry. The aim of the particle filter is the sequential estimation of state variables, by using a large set of random samples. Uncertainties are taken into account the evolution model, as well as in measurements. Simulated temperature measurements are used in the inverse analysis with RF heating and with iron oxide nanoparticles (Fe_3O_4). A 2D domain involving a complex geometry was considered for the analysis. The forward problem was solved by the finite element method (FEM) with Comsol Multiphysics® 5.0. The particle filter used for the solution of the inverse problem was coded in Matlab®.

STATE ESTIMATIOM PROBLEM

In order to define the state estimation problem, consider a model for the evolution of the vector **x** in the following form (Arulampalam et al. 2002):

$$\mathbf{x}_k = \mathbf{f}_k(\mathbf{x}_{k-1},\mathbf{v}_{k-1}) \tag{1}$$

where the subscript k = 1, 2, . . ., denotes a time instant t_k in a dynamic problem. The vector $\mathbf{x} \in R^{n_x}$ is called the state vector and contains the variables to be dynamically estimated. This vector advances in accordance with the state evolution model given by Eq. (1), where **f** is, in the general case, a nonlinear function of the state variables **x** and of the state noise vector $\mathbf{v} \in R^{n_v}$.

Consider also that measurements $\mathbf{z} \in R^{n_z}$ are available at t_k, k = 1, 2, ... The measurements are related to the state variables **x** through the general, possibly nonlinear, function **h** in the form.

$$\mathbf{z}_k = \boldsymbol{h}_k(\mathbf{x}_k,\mathbf{n}_k) \tag{2}$$

where $\mathbf{n} \in R^{n_n}$ is the measurement noise. The state estimation problem aims at obtaining information about $\mathbf{x}_k$ based on the state evolution model described in Eq. (1) and on the measurements $\mathbf{z}_{1:k}=\mathbf{z}_i$, i = 1, ..., k given by the observation model described in Eq. (2) (Arulampalam et al. 2002; Kaipio & Somersalo 2004; Maybeck 1979).

The evolution-observation model given by Eqs. (1-2) are based on the following assumptions (Kaipio & Somersalo 2004; Maybeck 1979):

i. The sequence $\mathbf{x}_k$ for k = 1, 2, ..., is a Markovian process, that is,

$$\pi\left(\mathbf{x}_k\middle|\mathbf{x}_0,\mathbf{x}_1,\ldots,\mathbf{x}_{k-1}\right) = \pi(\mathbf{x}_k|\mathrm{x}_{k-1}) \tag{3}$$

ii. The sequence $\mathbf{z}_k$ for k = 1,2, ..., is a Markovian process with respect to the history of $\mathbf{x}_k$, that is,

$$\pi\left(\mathbf{z}_k\middle|\mathbf{x}_0,\mathbf{x}_1,\ldots,\mathbf{x}_{k-1}\right) = \pi(\mathbf{z}_k|\mathbf{x}_k) \tag{4}$$

iii. The sequence $\mathbf{x}_k$ depends on the past observations only through its own history, that is,

$$\pi\left(\mathbf{x}_k\middle|\mathbf{x}_{k-1},\mathbf{z}_{1:k-1}\right) = \pi(\mathbf{x}_k|\mathbf{x}_{k-1}) \tag{5}$$

where $\pi(a|b)$ denotes the conditional probability of a when b is given. In addition, for the evolution-observation model given by Eqs. (1-2) it is assumed that for $i \neq j$ the noise vectors $\mathbf{v}_i$ and $\mathbf{v}_j$, as well as $\mathbf{n}_i$ and $\mathbf{n}_j$, are mutually independent and also mutually independent of the initial state $\mathbf{x}_0$. The vectors $\mathbf{v}_i$ and $\mathbf{n}_j$ are also mutually independent for all i and j (Kaipio & Somersalo 2004).

Different problems can be considered with the above evolution-observation model, namely: the prediction problem, concerned with the determination of $\pi(\mathbf{x}_k|\mathbf{z}_{1:k-1})$; the filtering problem, concerned with the determination of $\pi(\mathbf{x}_k|\mathbf{z}_{1:k})$; the fixed-lag smoothing problem, concerned with the determination of $\pi(\mathbf{x}_k|\mathbf{z}_{1:k+p})$, where $p \geq 1$ is the fixed lag; and the whole-domain smoothing problem, concerned with the determination of $\pi(\mathbf{x}_k|\mathbf{z}_{1:K})$, where $\mathbf{z}_{1:K} = \mathbf{z}_i$, i = 1, 2, ..., K is the complete sequence of measurements (Kaipio & Somersalo 2004).

This paper deals only with the filtering problem. By assuming that $\pi(\mathbf{x}_0|\mathbf{z}_0) = \pi(\mathbf{x}_0)$ is available, the posterior probability density $\pi(\mathbf{x}_k|\mathbf{z}_{1:k})$ is then obtained with Bayesian filters in two steps (Arulampalam et al. 2002; Kaipio & Somersalo 2004; Maybeck 1979): prediction and update, as illustrated in Fig. 1.

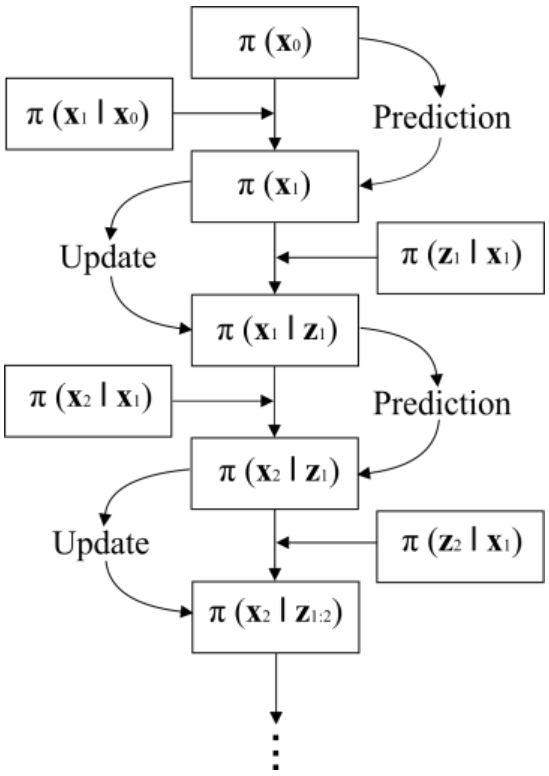

Figure 1: Prediction and Update Steps for State Estimation Problem (Kaipio & Somersalo 2004)

The Particle Filter method it is a Monte Carlo technique, where the required posterior density function is represented by a set of random samples with associated weights; the statistics of the posterior distribution is computed based on these samples and weights. The particle filter algorithms generally make use of an importance density, which is a density proposed to represent another one that cannot be computed exactly, that is, the sought posterior density in the present case. Then, samples are drawn from the importance density instead of the actual density (Andrieu & Doucet 2002; Kaipio & Somersalo 2004; Ristic et al. 2004).

We denote the particles, $\mathbf{x}_{0:k}^{i}$, with associated weights $w_k^i, i = 0,\ldots,N$ and the set of all state variables $\mathbf{x}_{0:k} = \{\mathbf{x}_j, j = 0,1,\ldots, k\}$ up to t_k, where N is the number of particles. The weights are normalized so that $\sum_{i=1}^{N} w_k^i=1$. Then, the posterior marginal distribution can be approximated by (Kaipio & Somersalo 2004; Ristic et al. 2004).

$$\pi(\mathbf{x}_k|\mathbf{z}_{1:k}) \approx \sum_{i=1}^{N} w_k^i \delta(\mathbf{x}_k-\mathbf{x}_k^i) \tag{6}$$

with weights computed from $w_k^i \propto w_{k-1}^i \pi(\mathbf{z}_k|\mathbf{x}_k^i)$ (Ristic et al. 2004).

The particle filter commonly presents a degeneracy phenomenon, where after a few states all but very few particles have negligible weight (Ristic et al. 2004; Kaipio & Somersalo 2004; Arulampalam et al. 2002). This problem can be overcome with a resampling step in the application of the particle filter. Resampling can be performed if the number of effective particles falls below a certain threshold number, or at every instant t_k, such as in the Sampling Importance Resampling (SIR) (Arulampalam et al. 2002; Ristic et al. 2004). In the SIR algorithm, resampling reduces the effects of degeneration, but the particles with larger weights are selected several times, which can result in a sample with many repeated particles, a phenomenon known as sample impoverishment. This undesirable effect is more significant when the state evolution model has low noise (Arulampalam et al. 2002). The Auxiliary Sampling Importance Resampling (ASIR) algorithm of the particle filter introduced by (Pitt & Shephard 1999) reduces sample impoverishment. Both the SIR and the ASIR algorithms are present in Table 1 and in Fig 2. Is illustrated the visualization of particle filter.

For the solution of the inverse problem, it is assumed here that the measurement errors are additive, uncorrelated, Gaussian random variables with zero means and known constant standard deviation, ν, and independent of the state variables. Thus, the likelihood function for each particle $\mathbf{x}_k^i$ can be expressed as (Ristic et al. 2004; Kaipio & Somersalo 2004; Arulampalam et al. 2002):

$$\pi(\mathbf{z}_k|\mathbf{x}_k^i)=(2\pi)^{-D/2}\nu^{-D}\exp\left\{-\frac{1}{2}\frac{[\mathbf{z}_k^{meas}-\mathbf{z}_k(\mathbf{x}_k^i)]^T[\mathbf{z}_k^{meas}-\mathbf{z}_k(\mathbf{x}_k^i)]}{\nu^2}\right\} \tag{7}$$

where $\mathbf{z}_k(\mathbf{x}_k^i)$ is obtained from the observation model given by equation (2) and D is the number of measurements.

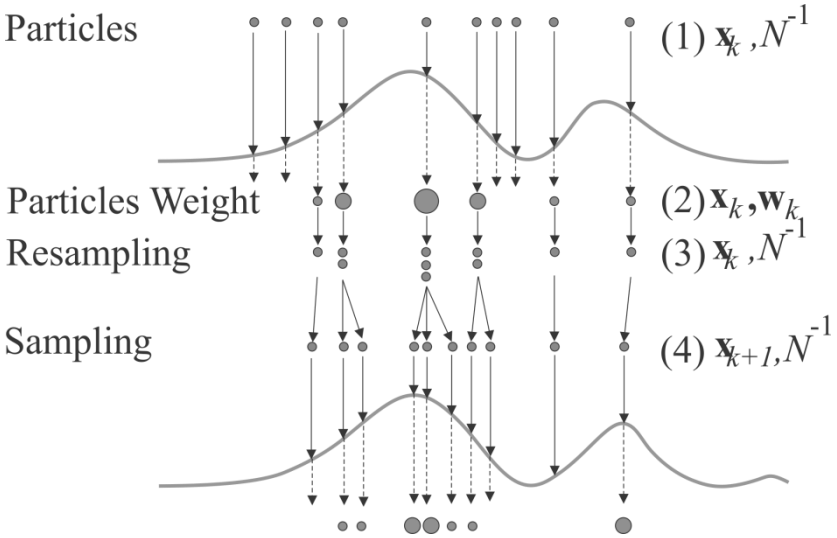

Figure 2: Particle Filter

Table 1 – Particles Filter Algorithm

SIR Algorithm	ASIR Algorithm
FOR $i = 1, \ldots, N$ $\mathbf{x}_k^i$ from the prior density $\pi(\mathbf{x}_k \mid \mathbf{x}_{k-1}^i)$ $w_k^i = \pi(\mathbf{z}_k \mid \mathbf{x}_k^i)$ using the likelihood density END FOR	FOR $i = 1, \ldots, N$ $\mathbf{x}_k^i$ from the prior density $\pi(\mathbf{x}_k \mid \mathbf{x}_{k-1}^i)$ calcule the expected value $\mu_k^i = \mathrm{E}[\mathbf{x}_k \mid \mathbf{x}_{k-1}^i]$ $w_k^i = \pi(\mathbf{z}_k \mid \mu_k^i) w_{k-1}^i$ using the likelihood density END FOR
Calculate the total weight $T_w = \sum_{i=1}^N w_k^i$	Calculate the total weight $T_w = \sum_{i=1}^N w_k^i$
FOR $i = 1, \ldots, N$ Normalize $w_k^i = T_w^{-1} w_k^i$ END FOR	FOR $i = 1, \ldots, N$ Normalize $w_k^i = T_w^{-1} w_k^i$ END FOR

Resample
$c_1 = 0$
FOR $i = 2, \ldots, N$
$c_i = c_{i-1} + w_k^i$, cumulative sum of weights (CSW)
END FOR
$i = 1$ draw a starting point u_1 from the $U[0, N^{-1}]$
FOR $j = 1, \ldots, N$
Move along the CSW by making $u_j = u_1 + N^{-1}(j-1)$;
WHILE $u_j > c_i$
$i = i + 1$
END WHILE
assign sample $\mathbf{x}_k^j = \mathbf{x}_k^i$
assign weight $w_k^j = N^{-1}$
END FOR
	Resample
	$c_1 = 0$
	FOR $i = 2, \ldots, N$
	$c_i = c_{i-1} + w_k^i$, cumulative sum of weights (CSW)
	END FOR
	$i = 1$ draw a starting point u_1 from the $U[0, N^{-1}]$
	FOR $j = 1, \ldots, N$
	Move along the CSW by making $u_j = u_1 + N^{-1}(j-1)$;
	WHILE $u_j > c_i$
	$i = i + 1$
	END WHILE
	assign sample $i^j = i$
	END FOR

	FOR $j = 1, \ldots, N$ $\mathbf{x}_k^j$ from the prior density $\pi(\mathbf{x}_k \mid \mathbf{x}_{k-1}^{i^j})$ $w_k^j = \frac{\pi(\mathbf{z}_k \mid \mathbf{x}_k^j)}{\pi(\mathbf{z}_k \mid \mu_k^{i^j})}$ using the likelihood density END FOR
	Calculate the total weight $T_w = \sum_{i=1}^N w_k^i$
	FOR $i = 1, \ldots, N$ Normalize $w_k^i = T_w^{-1} w_k^i$ END FOR

RF HYPERTHERMIA USING NANOPARTICLES

The physical problem considered in this paper involves a 2D complex domain that consists of different biological healthy tissues, with a tumor loaded of iron oxide nanoparticles. Thermophysical properties in the tissues are constant and two external electrodes for induction of radiofrequency are considered.

The electric potential within the domain can obtained by solving the following Laplace's equation (Cheng 1993).

$$\nabla\cdot[\varepsilon(\mathbf{X})\cdot\nabla\varphi(\mathbf{X})]=0 \tag{8}$$

where φ is the potential; ε is the permittivity, which varies spatially depending on the tissue. **X** are the Cartesian coordinates.

The interfaces between the tissues are assumed to have ideal electric contact. The boundary conditions on the surface of the domain are given by:

$$\varphi(\mathrm{X}) = U \quad \text{at } \Omega' \tag{9}$$

$$\frac{\partial\varphi(\mathrm{X})}{\partial n}=0 \qquad \text{at } \mathrm{X}\notin\Omega' \tag{10}$$

where U denote the electric potential with respect to ground.

The electric field strength **E** is obtained by:

$$\mathbf{E}(x,y,z) = -\nabla\varphi(\mathrm{X}) \tag{11}$$

while the intensity of the magnetic field **H** is obtained by (Andra et al. 1999):

$$|\mathbf{H}(\mathrm{X})|=\frac{1}{1+N(\chi)}\frac{|\mathbf{E}(X)|}{\mu_o\pi fR} \tag{12}$$

where $N(\chi)$=1/3 is the demagnetizing factor of the composite tissue (Andra et al. 1999; Lv et al. 2005), χ is the susceptibility of the magnetic nanoparticles that can be described in terms of complex susceptibility this is $\chi = \chi' + i\chi''$ (Rosensweig 2002; Pankhurst et al. 2003), μ_o is the dielectric constant permeability of free space (μ_o=4π x 10^{-7}T·m·A^{-1}), f is the electromagnetic frequency and R is the radius of magnetic induction loop.

The electric heat source in the tissues that do not contain nanoparticles is given by (Cheng 1993):

$$Q_{e_x}(\mathrm{X})=\frac{\sigma_x|\mathbf{E}(\mathrm{X})|^2}{2} \tag{13}$$

where σ_x is the electric conductivity of the biological healthy tissue.

The contribution for the electric heat source resulting from the presence of the magnetic nanoparticles is (Rosensweig 2002):

$$Q_n=\mu_0\pi f\chi''|\mathbf{H}(\mathrm{X})|^2 \tag{14}$$

Thus, the heat source in the tumor due to induction of magnetic nanoparticles can be calculated by (Andra et al. 1999):

$$Q_{e_y}(\mathrm{X})=\left(1-\theta\right)\frac{\sigma_y|\mathbf{E}(\mathrm{X})|^2}{2}+\theta\left(\frac{9}{16}\frac{\chi''}{\mu_o\pi fR^2}|\mathbf{E}(\mathrm{X})|^2\right) \tag{15}$$

where $\theta=n\pi r^2/A$ is the concentration of nanoparticles, r is the mean radius of the supposedly spherical nanoparticles, n is the number of nanoparticles, A is the area of the tumor and σ_y is the electrical conductivity of the tumor embedded with nanoparticles, which can be approximated by a serial arrangement of the two materials, this is, $1/\sigma_y=(1-\theta)/\sigma_y'+\theta/\sigma_n$, where σ_y' and σ_n are the electrical conductivity of tumor and nanoparticles, respectively. The permittivity of the tumor tissue embedded with nanoparticles is approximated by $\varepsilon_2=\varepsilon_2'$, where ε_2' is permittivity of the tumor, since the concentration of particles is too small and differences in this parameter for biological tissue and nanoparticles are not evidently large.

The mathematical formulation for bioheat transfer in this study is described by Pennes's Equation (Pennes 1948):

$$\rho C\frac{\partial T(\mathbf{X},t)}{\partial t} = \nabla\cdot[k\nabla T(X,t)] - \omega_b(X)\rho_b C_b T(X,t) + Q(X,t) \tag{16}$$

where ρ is the density, C is the specific heat, T is the temperature, k is the thermal conductivity, ω_b is the blood perfusion rate, ρ_b is the blood density, C_b is the specific heat of blood and Q is the heat source given by:

$$Q = \omega_b(\mathrm{X})\rho_b C_b T_b(\mathrm{X}) + Q_m(\mathrm{X}) + Q_e(\mathrm{X}) \tag{17}$$

where T_b is the blood temperature, Q_m is the metabolic heat source and Q_e is the heat source generated by external electromagnetic excitation.

The interfaces between biological healthy tissues are assumed to be in ideal thermal contact and the thermal boundary conditions are given by:

$$\begin{cases} -k\frac{\partial T(x,y)}{\partial x} = 0 & \text{at } x=0,\ x=L_x,\ 0 < y < L_y, t > 0 \\ -k\frac{\partial T(x,y)}{\partial y} = h_f\left(T(x,y)-T_f\right) & \text{at } y=0,\ y=L_y,\ 0 < x < L_x, t > 0 \end{cases} \tag{18}$$

where h_f is the heat transfer coefficient, T_f is the temperature of the surrounding medium, L_x and L_y are the domain lengths in the x and y directions, respectively. The initial temperature T_0 is considered constant.

RESULTS AND DISCUSSIONS

A 2D complex domain has been considered in this work, containing muscle, fat, lungs, pancreas, small intestine, arteries and vertebrae. A tumor is located inside the pancreas; the tumor is loaded with nanoparticles of iron oxide (Fe_3O_4). The lengths of both electrodes are 20 cm. as the physical domain is illustrated by Fig. 3.

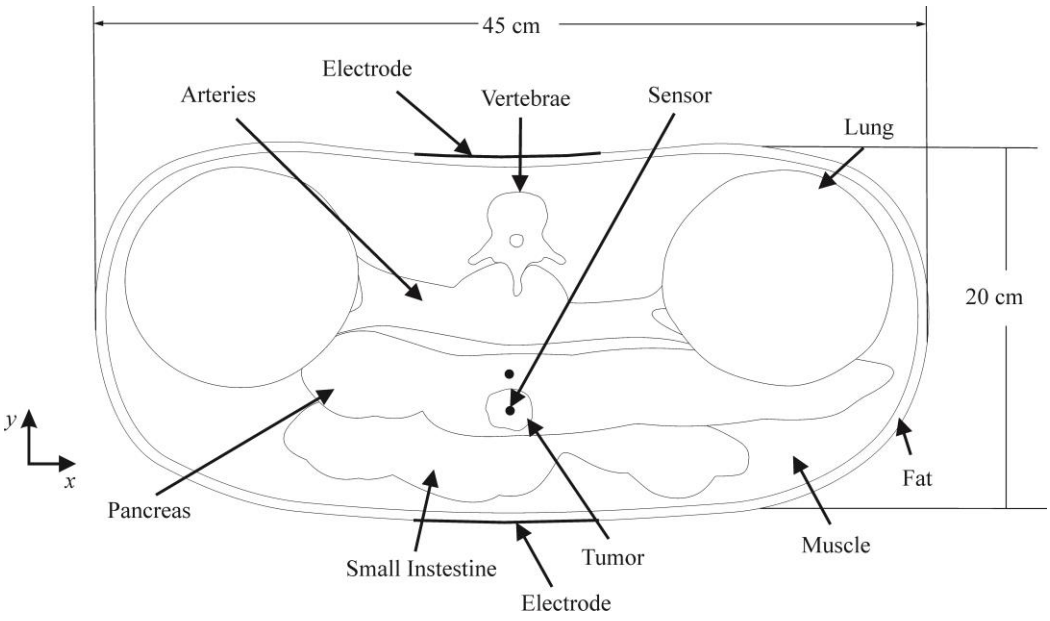

Figure 3: System Domain

Thermophysical properties of the biological healthy tissues and tumor, and the electrical properties considering a frequency f = 1 MHz are described in Table 2. For the convective boundary condition we assume T_f = 20°C, and h_f = 45 W/(m^{2}K). The initial condition is taken as the uniform temperature T_0 = 37°C. For the iron oxide nanoparticles (Fe_3O_4) that are assumed to be uniformly distributed into the tumor, the following parameters have been considered: k_n = 40 W/(mK), C_n = 4000 J/(kgK), ρ_n = 5180 kg/m^3 , σ_n = 25000 S/m, $\varepsilon_n = \varepsilon_y$ and magnetic susceptibility $\chi'' = 18$, with n = 10^8 nanoparticles of radius r = 10^{-8} m (Lv et al. 2005). The properties for the tumor embedded with nanoparticles was approximated by the rule of mixture (Andra et al. 1999).

Table 2 – Thermophysical and Electrical Properties (Hasgall et al. 2015)

Parameter	Pancreas	Small Intestine	Lung	Muscle	Fat	Vertebrae	Arteries	Tumor
Thermal Conductivity (k) W/(m.K)	0.51	0.49	0.39	0.49	0.21	0.32	0.46	0.75[2]
Specific Heat (C) J/(kgK)	3164	3595	3886	3421	2348	1313	3306	3164[1]
Density (ρ) kg/m^3	1087	1030	394	1090	911	1908	1102	1087[1]
Perfusion Coefficient (ω) s^{-1}	0.01389	0.01761	0.00263	0.0006	0.0005	0.0003	0.0027	0.02
Metabolic Heat Source (Q_m) W/m^3	12924.43	16366.7	2446.74	991.9	464.61	286.2	2556.64	42000[2]
Electrical Conductivity (σ) S/m	0.603	0.865	0.136	0.503	0.0441	0.00244	0.327	0.723[2]
Permitivitty (ε)	1430	5680	733	1840	50.8	145	218	1716[2]

[1] thermal properties of pancreas. [2] (Paruch 2014)

The forward problem solution is analyzed without and with nanoparticles of Fe_3O_4, with a voltage on the top electrode of 10V with respect to the other electrode maintained to ground, during 900s. Figure 4 presents the transient temperature inside the tumor, at the position x = 22.5 cm and y = 5 cm. For the case without nanoparticles, the maximum temperature is 38.78°C, and the temperature increase does not reach levels of hyperthermia. For the case with nanoparticles inside tumor, the maximum temperature is 44.34°C, which, reveals that the use of nanoparticles in the tumor increase the temperature substantially in this region while keeping the other regions at lower temperatures (see also Figure 5 for the temperature in the pancreas, outside the tumor, at the position x = 22.5 cm and y = 7 cm.

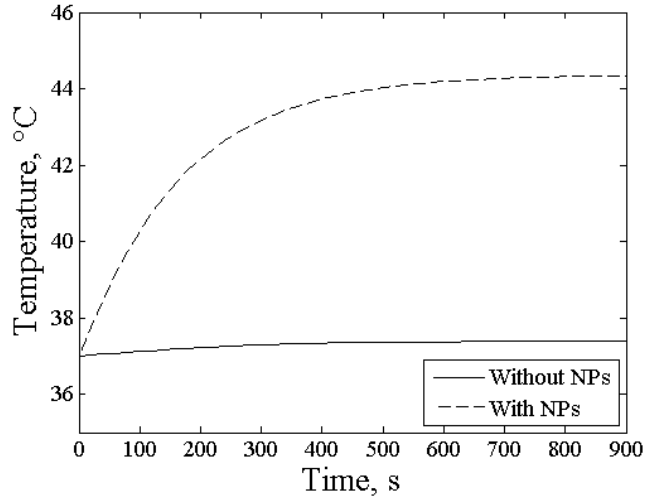

Figure 4: Transient Temperature in Tumor

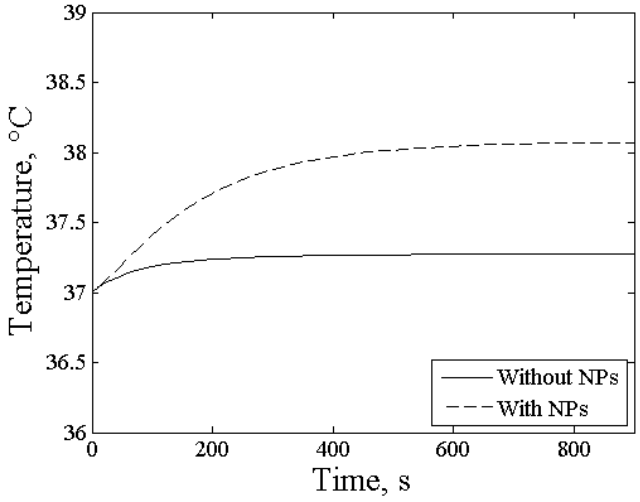

Figure 5: Transient Temperature in Pancreas

For the solution of the state estimation problem, one single sensor was assumed available for the inverse analysis, located inside the tumor. The measurements were generated from the solution of the forward problem with the parameters specified above. Uncorrelated Gaussian errors with zero mean and standard deviation of 1°C were then added to the solution. The simulated measurements were supposed available every 20s.

The evolution model for the electrical volumetric heat source was taken in the form of a random walk, that is, for each particle *i*

$$Q^{i}_{e,k}(x,y)=Q^{i}_{e,k-1}(x,y)+\xi^{i}_{e,k}(x,y) \tag{19}$$

where $\xi^{i}_{e,k}(x,y)$ is a Gaussian random variable with zero mean and a standard deviation of 10% of the deterministic solution of the electrical problem. The subscript k in equation (19) does not represent a time evolution of $Q_e(x,y)$, but the fact that it is treated as state variable for the application of the particle filter that aims at the estimation of the electric heat source and of the transient temperature field, at each position (x,y) of each finite-element used for the numerical solution of the coupled electric and bioheat transfer problem. The particles $Q^{i}_{e,0}(x,y)$ at each position (x,y) were initially sampled from Gaussian distributions with means obtained from the deterministic solution of the electric problem and with standard deviations of 10% of these means.

In the evolution model for temperature field, a Gaussian uncorrelated noise with zero mean and a standard deviation of 1°C was added to the solution of the bioheat transfer problem, which was solved with each sample of the Gaussian distribution of the electrical heat source.

SIR and ASIR algorithms of the particle filter, with 50, 100 and 200 particles, were used and 30 repetitions were performed for each estimation, in order to compute the RMS defined by Eq. (20).

$$\text{RMS}=\sqrt{\frac{1}{M}\sum_{i=1}^{M}\left[x_{est}(i)-x_{exa}(i)\right]^{2}} \tag{20}$$

where x_{est} represents the estimated values, x_{exa} represents the exact values and M is the total number of points used in the analysis of the RMS error. Table 3 shows the means and standard deviation values of the 30 repetitions of the particle filter, for each case examined here. We note that the ASIR filter presents a better performance in terms of the accuracy of the prediction than the SIR filter, even with a small number of particles.

Table 3 – RMS Results

Filter	Number of Particles	$\overline{\text{RMS}}$	Standard Deviation
SIR	50	0.765	0.390
	100	0.618	0.297
	200	0.525	0.234
ASIR	50	0.623	0.398
	100	0.601	0.315
	250	0.512	0.298

Figure 6 shows the transient temperature at the tumor obtained with the SIR filter with 50 particles, where we note that the estimated temperature is in better agreement with the exact solution than the measurements. Figure 7 presents the transient temperature inside the pancreas, in a position where no measurements are available. Also, for this position, it is observed that the estimated temperature is in excellent agreement with the exact temperature. We note in table 3 that the results presented by figures 6 and 7 correspond to the case with the largest RMS errors; hence, we note in these figures that, even for this case, the temperatures can be quite accurately estimated.

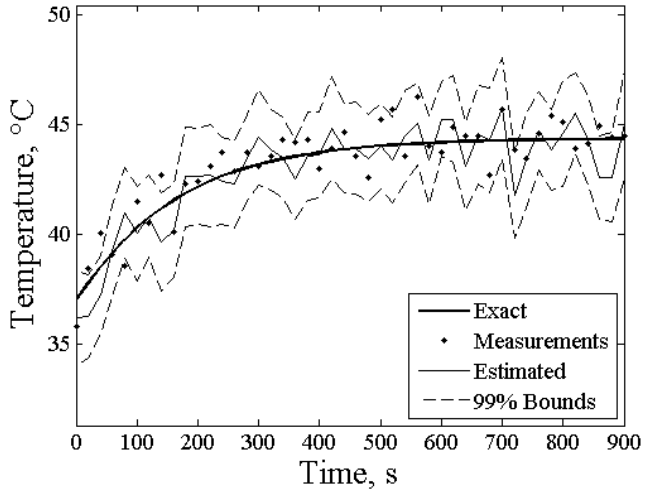

Figure 6: Estimated Temperature at Sensor Position

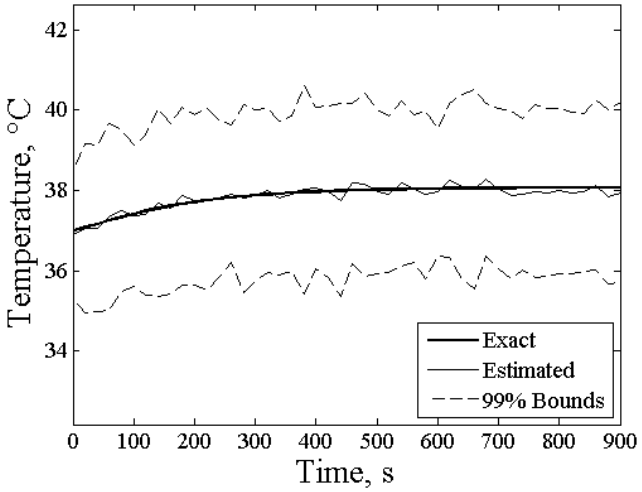

Figure 7: Estimated Temperature at Pancreas

CONCLUSIONS

The accuracy of the SIR and ASIR particle filter algorithms, as applied to the estimation of the temperature field in RF hyperthermia with nanoparticles of iron oxide, with one single measurement point, on a 2D complex geometry, was analyzed for 50, 100 and 200 particles. Excellent results were obtained for the estimated temperature in the whole region, even in locations where no measurements are available. The results presented herein are expected to contribute for future temperature control in the hyperthermia treatment and for establishing a protocol for optimal performance.

ACKNOWLEDGMENTS

The authors are thankful for the support provided by CNPq, CAPES and FAPERJ, Brazilian agencies for the fostering of science.

REFERENCES

Andra, W. et al., 1999. "Temperature distribution as function of time around a small spherical heat source of local magnetic hyperthermia". Journal of Magnetism and Magnetic Materials, 194, pp.197–203.

Andrieu, C. and Doucet, A., 2002. Particle filtering for partially observed Gaussian state space models. Journal of the Royal Statistical Society: Series B Statistical Methodology, 64(4), pp.827–836.

Arulampalam, M.S. et al., 2002. "A tutorial on particle filters for online nonlinear/non-Gaussian Bayesian tracking". IEEE Transactions on Signal Processing, 50(2), pp.174–188.

Cheng, D.K., 1993. Fundamentals of Engineering Electromagnetics, United State of America: Addison-Wesley Publishing Company, Inc.

Colombo, R. et al., 2003. "Multicentric study comparing intravesical chemotherapy alone and with local microwave hyperthermia for prophylaxis of recurrence of superficial transitional cell carcinoma". Journal of clinical oncology : official journal of the American Society of Clinical Oncology, 21(23), pp.4270–6. Available at: http://www.ncbi.nlm.nih.gov/pubmed/14581436 [Accessed September 17, 2013].

Costa, J.M.J. et al., 2015. "Estimation of Tumor Size Evolution Using Particle Filters". Journal of Computational Biology, 22(7), pp.1–17.

Dombrovsky, L. a. et al., 2011. "A Combined Transient Thermal Model for Laser Hyperthermia of Tumors with Embedded Gold Nanoshells". International Journal of Heat and Mass Transfer, 54(25-26), pp.5459–5469.

Dombrovsky, L. a. et al., 2015. "Radiative heating of superficial human tissues with the use of water-filtered infrared-A radiation: A computational modeling". International Journal of Heat and Mass Transfer, 85(JUNE), pp.311–320. Available at: http://linkinghub.elsevier.com/retrieve/pii/S0017931015001519.

Eibner, S. et al., 2014. "Near Infrared Light Heating of Soft Tissue Phantoms Containing Nanoparticles". Engenharia térmica, 13, pp.13–18.

Hasgall, P.. et al., 2015. "IT'IS Database for thermal and electromagnetic parameters of biological tissues". Version 3.0.

Horsman, M.R. and Overgaard, J., 2007. "Hyperthermia: a potent enhancer of radiotherapy". Clinical oncology (Royal College of Radiologists (Great Britain)), 19(6), pp.418–26.

Kaipio, J.P. and Somersalo, E., 2004. Computational and Statistical Methods for Inverse Problems, Berlin, Heidelberg: Springer.

Kurgan, E. and Gas, P., 2015. "Simulation of the electromagnetic field and temperature distribution in human tissue in RF hyperthermia". Przeglad Elektrotechniczny, 1(1), pp.171–174.

Lamien, B. et al., 2014. "State Estimation Problem in Hyperthermia Treatment of Tumors Loaded with Nanoparticles". In Proceedings of the 15th International Heat Transfer Conference, IHTC-15. Kyoto, Japan, pp. 1–15.

Lv, Y.-G., Deng, Z.-S. and Liu, J., 2005. "3-D numerical study on the induced heating effects of embedded micro/nanoparticles on human body subject to external medical electromagnetic field". IEEE transactions on nanobioscience, 4(4), pp.284–294.

Maybeck, P., 1979. Stochastic Models, Estimation, and Control Academic Press Inc, ed., NY, USA.

Miaskowski, A. and Sawicki, B., 2013. "Magnetic fluid hyperthermia modeling based on phantom measurements and realistic breast model". IEEE transactions on bio-medical engineering, 60(7), pp.1806–13.

Ng, E.Y.K. and Jamil, M., 2014. "Parametric sensitivity analysis of radiofrequency ablation with efficient experimental design". International Journal of Thermal Sciences, 80(1), pp.41–47.

Pankhurst, Q.A. et al., 2003. "Applications of magnetic nanoparticles in biomedicine". Journal of Physics D: Applied Physics, 36(13), pp.R167–R181.

Paruch, M., 2014. "Hyperthermia process control induced by the electric field in order to cancer destroying". Acta of Bioengineering and Biomechanics, 16(4), pp.123–130.

Pennes, H.H., 1948. "Analysis of tissue and arterial blood temperatures in the resting human forearm". 1948. Journal of applied physiology, 1(2), pp.93–124.

Pitt, M.K. and Shephard, N., 1999. "Filtering via Simulation: Auxiliary Particle Filters". Journal of the American Statistical Association, 94(446), pp.1–41.

Ristic, B., Arulampalam, M.S. and Gordon, N., 2004. Beyond the Kalman Filter, Boston, MA: Artech House.

Rosensweig, R.E., 2002. "Heating magnetic fluid with alternating magnetic field". Journal of Magnetism and Magnetic Materials, 252, pp.370–374.

Varon, L.A.B., Orlande, H.R.B. and Elicabe, G., 2015. "Estimation of state variables in the hyperthermia therapy of cancer with heating imposed by radiofrequency electromagnetic waves". International Journal of Thermal Sciencies, 98, pp.228–236.

RESPONSIBILITY NOTICE

The authors are the only responsible for the material included in this paper.